

# Formation of ‘Super Plastic Agglomerate Mixing’ (SPAM) Between Copper and 6061-T6511 Aluminum Deposited by the Supersonic Particle Deposition Process (SPD)

Victor K. Champagne, Jr.  
Dennis Helfritch  
Phillip Leyman  
Scott Grendahl  
Brad Klotz

US Army Research Laboratory  
Weapons and Materials Directorate  
Aberdeen Proving Ground, Aberdeen, MD 21005-5069

**Abstract:** Supersonic Particle Deposition (SPD) is a process whereby metal powder particles are utilized to form a coating by means of ballistic impingement upon a suitable substrate. The metal powders range in particle size from <5 –50 microns and are accelerated by a supersonic (300-1000 m/s) stream of compressed gas. The spray nozzle design incorporates the use of a converging-diverging throat through which a preheated gas stream is expanded to attain supersonic velocities, with an accompanying decrease in temperature. The term “cold spray” has been used to describe this process due to the relatively low temperatures (0-500°C) of the expanded gas particle stream that exits the nozzle, but within the context of this paper the process will be referred to as ‘Supersonic Particle Deposition’ or SPD, which the authors feel best describe this process. The adhesion of the metal powder to the substrate, as well as the cohesion of the deposited material, is accomplished in the solid state and the characteristics of the SPD deposit are quite unique, having significant advantages over thermal spray methods. The SPD process does not use thermal energy to melt the particles to be deposited, but instead relies upon the supersonic impact of the particles on the substrate, which plastically deform and cause cratering. The bonding mechanism of SPD has been theorized to be analogous to that of explosive welding, whereas the formation of a solid-state jet of metal occurs at the impact point between the particle and

the substrate. The objective of this paper is to present microstructural evidence of such a bonding mechanism, introduced as ‘Super Plastic Agglomerate Mixing’ (SPAM), between copper and Al6061-T6511 deposited by SPD. Measurements of adhesion strength, hardness and density of the SPD coating are included and the process parameters that are required to produce SPAM will also be discussed.

**Key Words:** Supersonic Particle Deposition, Cold Spray, Coatings, Characterization of Coatings

## The ARL SPD System

A schematic of the SPD system is shown in Figure 1.

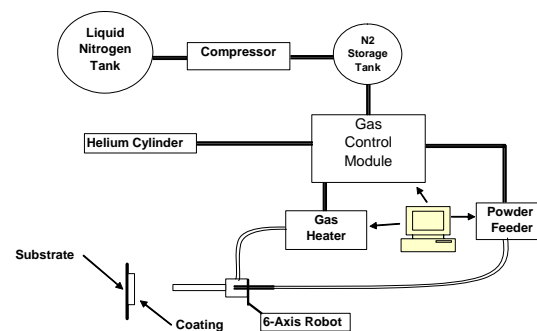


**Figure 1. Schematic of Supersonic Particle Deposition System.**

The system consists of a compressor to provide high pressure gas to both the main heated gas line and the powder feed line.

The main gas stream passes through electrically heated tubing that heats the gas to 300-500C. The Praxair Model 1264HPHV high pressure high volume powder feeder with a 240-hole wheel provides controlled metering of the powder into the gas stream of the powder gas stream. These two gas streams are combined in a manifold immediately prior to the nozzle where the particles are heated and subsequently accelerated to supersonic speeds via a diverging-converging nozzle design. The gas control module, gas heater and the powder feeder are interfaced via Ethernet connections to the computer control system to control the temperature and pressure of the gas streams in addition to the powder feed rate. The computer control system provides not only real time monitoring of these parameters but the data is continuously collected and stored and available for subsequent analysis. The uniformity of the coating is controlled by a fully programmable Motoman UP20 6-axis robotic system.

**Substrate Material**

The substrate material used in this study is 6061-T6511 aluminum. The typical dimensions of the substrate was 3.0” x 1.5” x 0.50” thick to facilitate performing the triple lug shear test. The typical composition of the aluminum as determined the DC plasma emission technique is listed in Table 1.

Elements	6061 Aluminum	500A Copper Powder
Aluminum	Balance	<0.005
Chromium	0.04 - 0.35	<0.005
Copper	0.15 - 0.4	99.85
Iron	0 - 0.7	0.005
Magnesium	0.8 - 1.2	<0.005
Manganese	0.15 max	<0.005
Silicon	0.4 - 0.8	<0.005
Titanium	0.15 max	-
Zinc	0.25 max	0.01

**Table 1. Typical chemical composition (by wt%) of substrate material.**

**Powder Material**

A spherical Copper powder (500A) from ACuPowder International LLC powder of 17um (typical) average particle size was used to generate the coating. It is an annealed powder which has a minimum purity of 99.3% copper with the specifications listed in Table 2.

	Average Particle Size – Microns (typical)		
	10% <sup>(1)</sup>	50% <sup>(2)</sup>	90% <sup>(3)</sup>
Cu Powder	8	17	28

- (1) 10% of particles are finer than stated Micron value
- (2) 50% of particles are finer than stated Micron value.
- (3) 90% of particles are finer than stated Micron value

**Table 2. Typical Particle Size Distribution of Copper Powder.**

The 500A copper powder was examined with a Hitachi S4700 Field Emission Scanning Electron Microscope (FSEM). Specimens were prepared by sprinkling the powder on wet carbon paint and gently blowing the excess powder from the surface. After the paint dried, the specimens were examined under the microscope.

The particles in Figure 2 are seen to be quite spherical. The software program analySIS® was used to determine the size distribution in each of the micrographs. This was accomplished by manually fitting a circle around each particle. The program then compiled a listing of the circle perimeters and areas. These listings were transferred to an Excel® spreadsheet where diameters were determined.

Particles were then grouped into bins according to their diameters and plotted. There were 1127 particles counted for the 5 micron powder and 464 particles for the 20 micron powder. The particle size distribution is shown in Figure 3.

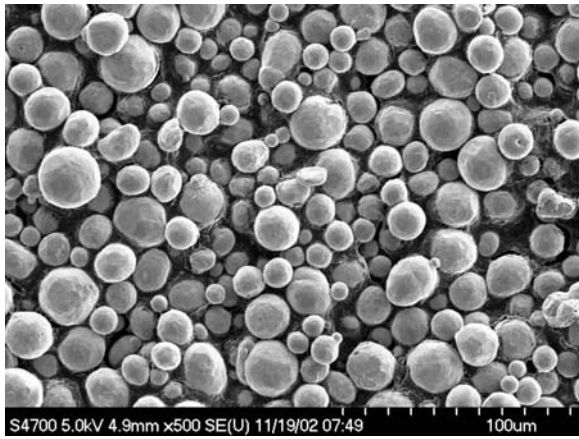


Figure 2. FSEM Photograph of Copper Powder.

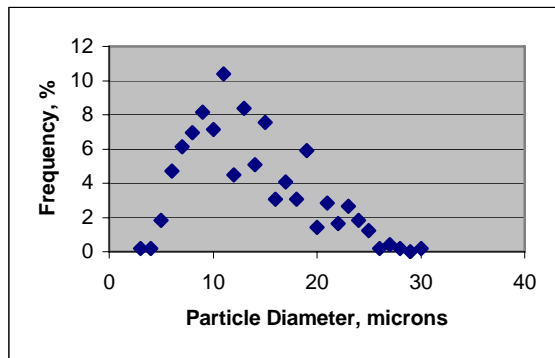


Figure 3. Copper Powder Size Distribution (Visual Method)

Next, a Horiba LA-910 laser scattering particle size distribution analyzer was used to determine the size distribution of the powder. This technique uses laser scattering from the particles suspended in solution to determine the distribution. Several measurements were made on the sample. In general, the measurements agreed with each other, so that only a representative measurement is shown in Fig. 4.

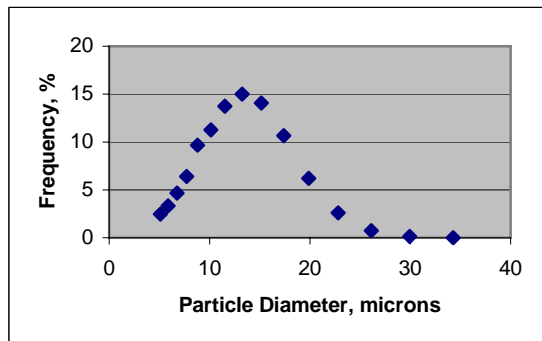


Figure 4. Copper Powder Size Distribution, Horiba LA-910.

## Feed Rate Correlation

Feed rate studies for the copper powder were conducted on the Praxair Model 1264HPHV Powder Feeder while connected to the SPD System to ascertain the feed rate of the 500A Copper powder. A 240-hole wheel is installed in the powder feeder to facilitate continuous pulse-free feeding of the copper powder. Tygon tubing was attached to the outlet of the SPD system nozzle to direct the powder flow to a container with a submicron filter on the outlet to capture the powder while allowing the gas to escape. The calculated feed rate is determined by using the apparent density of copper and the volume of the cavities in the 240-hole powder wheel. The feed rate data comparing the measured feed rate with the calculated data is presented in Figure 5. This not only shows excellent correlation between the actual and theoretical data but that the Praxair powder feeder with the 240-hole wheel gives a very reproducible feed rate.

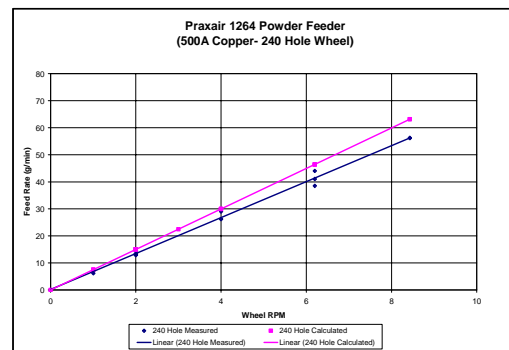


Figure 5. Plot of Measured Feed Rate Compared to Calculated Data.

## Process Parameters & Characterization

The aluminum substrates were placed from 15 to 35mm from the nozzle exit aperture and coated with copper to approximately 1 mm in thickness using the process parameters listed in Table 3. The coatings were deposited using nitrogen for both the heated gas and powder carrier gas. The powder carrier gas was maintained at either

10 or 20 psi greater than the heated gas. An area covering 1.85” by 1.5 “ of the aluminum block was coated in a raster pattern at the specified traverse speed with an index of 1.0mm between passes.

Trial	# 1	#2	#3	#4
Feed Rate (gm/min)	7	28	28	7
Main Gas Pressure (psi)	280	280	380	380
Delta Gas Pressure (psi)	20	10	10	20
Temp (C)	450	350	450	350
Standoff Distance (mm)	35	15	35	15
Traverse Speed (mm/s)	50	50	10	10
Coating Thickness (mm)	1.02	1.02	1.14	1.09

**Table 3. Deposition Parameters and Coating Thickness**

Two levels of each variable were employed to evaluate the effect of each of the parameters on coating hardness and bond strength. The final coating thickness was maintained at approximately 1 mm to reduce any potential effect that this might have on the resultant hardness and bond strength tests.

### Hardness Testing

The coatings were machined flat and smooth utilizing a milling machine prior to hardness testing. Hardness measurements were performed on the coatings using a Wilson Instruments Model C524-T Rockwell Hardness Tester. Nine measurements were taken in a 3/4” diameter circular pattern on each coating. Rockwell B tests results using a 1/16” ball at a 100kg major load and a 10 kg minor load are reported in Table 4.

### Bond Strength Testing

Since the bonding mechanism of the particular substrate/coating combination was theorized to be analogous to explosive

bonding, conventional means of testing bond strength could not be used because the bond strength would exceed the of the glues used for standard tensile strength measurements

Trial	Average	Standard Deviation
1	71.1	0.9
2	76.7	1.83
3	69.9	0.61
4	67.5	1.02

**Table 4. Rockwell B Hardness Results for Copper Coatings.**

(10-12 ksi). Therefore an alternative method for determining the bond strength was employed. The Triple Lug Shear Test method which is specifically designed for bimetallic joints formed by roll bonding and explosive bonding processes was used to determine the adhesion of the copper coating to the aluminum substrate. The Triple Lug procedure for the test method is prescribed in military specification, MIL-J-24445A.

A photograph of the actual copper coating machined to form three rectangular lugs measuring 1” by 0.2” as specified in Figure 5 of MIL-J-24445A which is shown in Figure 7.

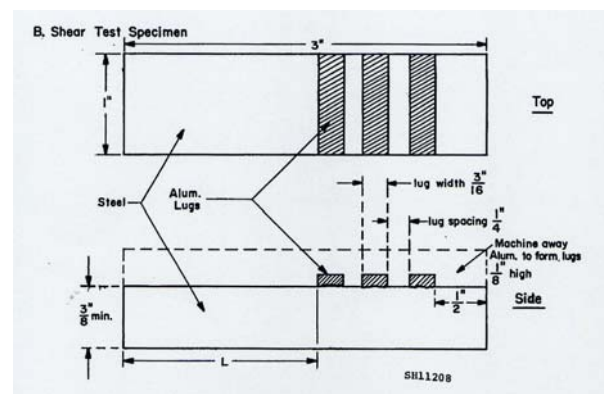


**Figure 6. Schematic of the Shear Test Specimen from MIL-J-24445A.**

A Shear Test Fixture was fabricated from that in the military specification shown in Figure 7. A photograph of the actual fixture with a copper coated aluminum block

inserted in the fixture for testing is shown in Figure 9.

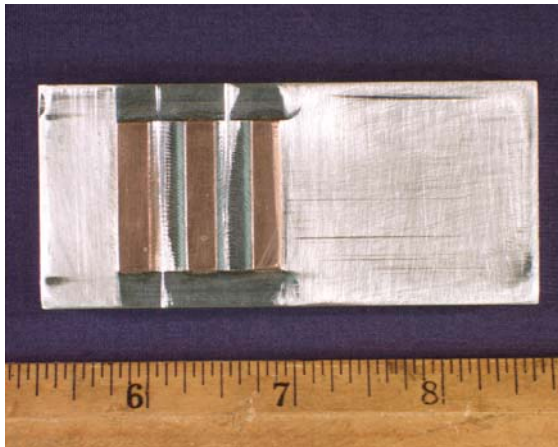


Figure 7. A Photograph of the copper coating machined to form three rectangular lugs for testing.

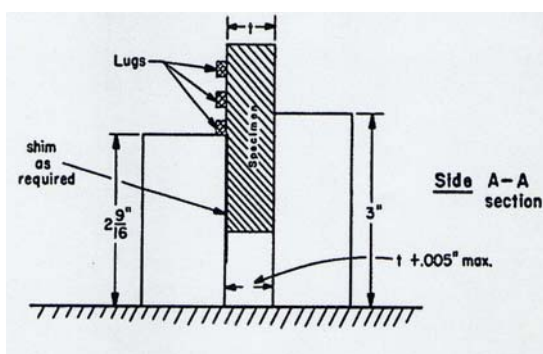


Figure 8. Schematic of the Shear Test Fixture from MIL-J-24445A.

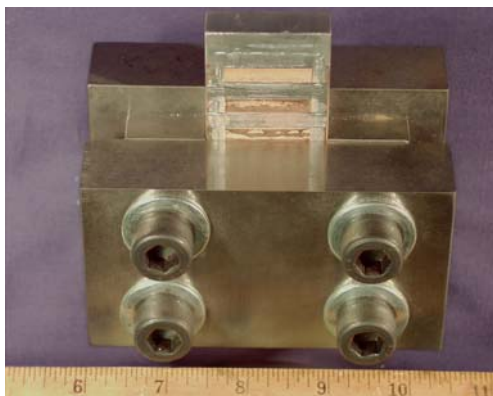


Figure 9. A Photograph of the Fabricated Triple Lug Shear Test Fixture with the Copper Coated Aluminum Block.

The triple lug shear tests were performed on an Instron 8500 Plus Dynamic Testing

System equipped with an Instron model 1331 Load Frame and controlled by a Series IX Automated Computer Program. The aluminum block with the three machined rectangular lugs was inserted into the fixture as shown in Figure 8. The fixture was then placed in the load frame of the Instron Testing System. The results are reported in Table 5.

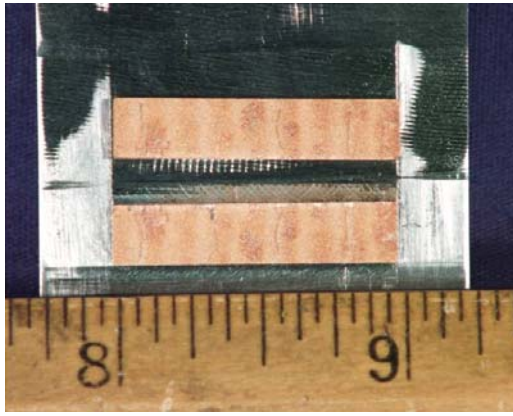
Trial	Lug #1	Lug #2	Lug #3	AVG
1	6520	6115	3405	5347
2	6400	5415	6400	6072
3	5520	5485	9045	6683
4	10825	9635	9710	10057

Table 5. Results of the Triple Lug Bond Strength Tests (lb/in<sup>2</sup>)



Figure 10. A Photograph of the Shear Test Fixture mounted on the Model 1331 Load Frame.

The test samples displayed a cohesive failure within the copper coating and not an adhesive failure at the interface between the copper coating and the aluminum substrate as shown in Fig. 11. This occurred in all of the samples sheared.



**Figure 11. Sheared Interface of the Lug after Shear Test (Sheared off piece is inverted above the copper coating remaining on the aluminum substrate)**

The coating that yielded the highest shear strength was trial #4 which was deposited at the higher nitrogen gas pressures for both the main gas and powder gas but at the lower conditions for all remaining parameters. Specifically, a coating with higher shear strength is produced when the copper powder is fed at a lower feed rate (7 gms/min), accelerated at a combined gas pressure of 400psi and heated to a temperature of 350C while closer to the substrate and traversing at a slower speed.

### The Prediction of Super Plastic Agglomerate Mixing (SPAM)

The bonding mechanism between particles and substrate and between particles and previously deposited particles created by the SPD process is considered to be caused by interfacial heating and plasma jet formation resulting from high velocity impact. In addition, the shear instability at the interface of the particles and substrate induces a wavy pattern at the interface. These behaviors are readily observable in explosive welding, where an explosive charge is used to drive two metals together at extremely high velocity. A typical bond<sup>1</sup> interface created by explosive welding is shown in Figure 12. The metals are zirconium on steel.

<sup>1</sup> A. Nobili, "Explosive Bond Process", Nobelclad Technical Bulletin NT 200, 2002

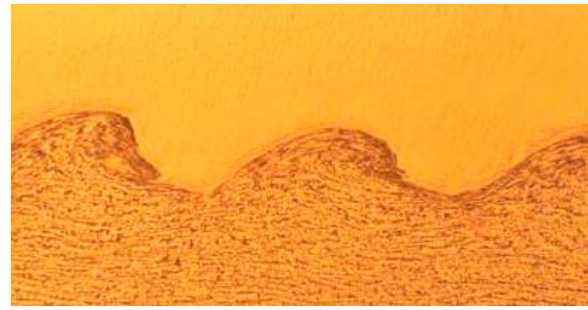


**Figure 12. Explosive bonding of zirconium on steel**

Figure 13 results when the behavior of a single particle impacting a substrate is modeled.<sup>2</sup> The computation uses the Zerilli-Armstrong (strain rate dependent) and the Steinberg-Guinan-Lund plastic models respectively for copper particles impacting an aluminum plate. In this case a 20 micron copper sphere impacting an aluminum plate at 650 m/second is modeled. A viscous jet is seen to form at the particle-substrate interface. The viscous, fluid-like nature of the jet can be expected to result in the

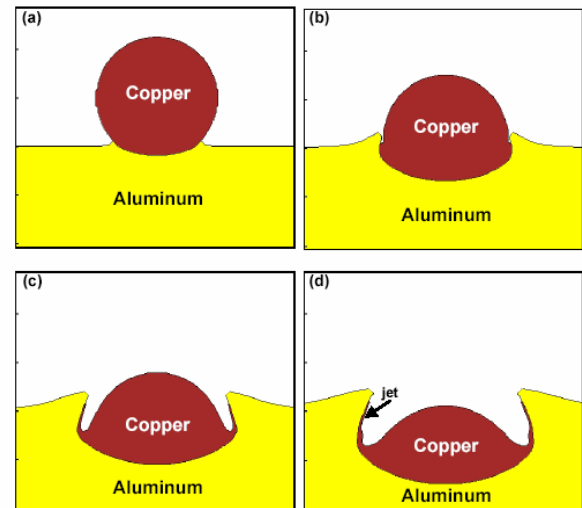


**Figure 13. Impact of a copper particle on a copper substrate at the times: (a) 5 ns (b) 20 ns (c) 35 ns (d) 50 ns.**

<sup>2</sup> M. Grujicic, J. Saylor, D. Beasley, W. DeRosset and D. Helfritch, "Computational Analysis of the Interfacial Bonding between Feed-Powder Particles and the Substrate in the Cold-Gas Dynamic-Spray Process", Applied Surface Science, accepted for publication, April 2003.

formation of interfacial waves, roll-ups and vortices.

The effect of projectile impact on substrates has been frequently estimated by means of semi-empirical equations. An empirical projectile penetration law by Eichelberger and Gehring<sup>3</sup> relates the crater volume produced by micrometeoroid impact on spacecraft. This is given by the equation:

$$\text{Volume} = 4 \times 10^{-9} E/B \quad 1$$

Where E is the projectile kinetic energy and B is the substrate Brinell Hardness. It is found<sup>4</sup> that this equation yields accurate results for velocities below 10 km/sec.

In order to make use of equation 1, we substitute  $1/2 mV^2$  for E and  $4/3\pi r^3\rho$  for m. We assume the crater volume is the particle area ( $\pi r^2$ ) times the penetration depth. The penetration depth is then given by:

$$L = 4 \times 10^{-9} (2\pi r/3)V^2/B \quad 2$$

If we assume that SPAM onset occurs when the particle is completely embedded at  $L = 2r$ , we can solve for the onset velocity:

$$V = (7.5 \times 10^8 B/\rho)^{0.5} \quad 3$$

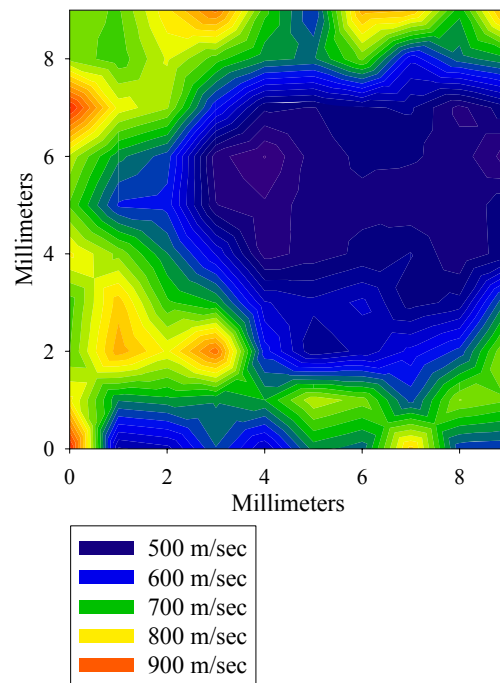
Where  $\rho$  is the particle density, given in gm/cc, and the velocity, V, is in cm/second.

Equation 3 gives us a simple, empirical, method to estimate the attainment of SPAM conditions. For copper particles impacting 6061 aluminum, equation 3 gives a SPAM onset velocity of 500 m/second. The actual particle velocities used during the creation of the sample of Figure 15 are shown in Figure 14. These velocities were measured

by the use of a DPV-2000, dual-slit, laser illuminated, optical sensor. This figure shows the velocity distribution in a plane perpendicular to the nozzle axis, 2.5 cm downstream of the nozzle exit. The plume centerline is at approximately 6,6 mm. It is seen that the core velocities are 500 m/second, with velocities reaching 900 m/second a few millimeters off the centerline. Clearly, the conditions for SPAM creation are satisfied.

### Microstructural Examination

Cross-sections of the copper SPD coatings were prepared for metallographic examination. Samples were sectioned with a diamond cut-off saw. Diamond polishing media and diamond suspension were utilized throughout the grinding, rough polishing and final polishing steps to avoid contamination.



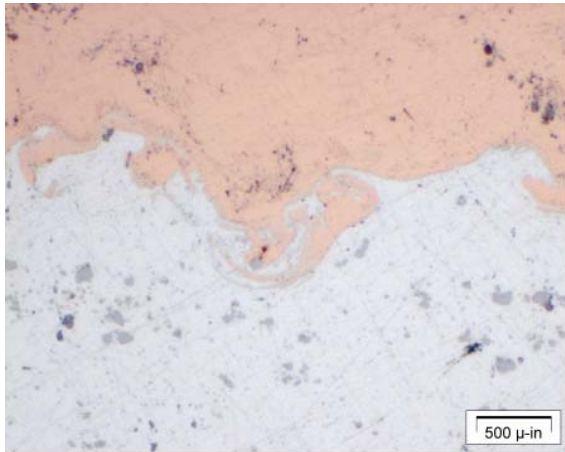
**Figure 14. SPD plume velocity distribution**

Figure 15 represents an as-polished cross section of the SPD copper coating. There is clear evidence of forced mixing between the deposited copper and the aluminum

<sup>3</sup> R. J. Eichelberger and J. W. Gehring, "Effects of Meteoroid Impacts on Space Vehicles," *ARS J.*, Vol. 32, No. 10, October 1963, p. 1583

<sup>4</sup> R. L. Bjork, "Review of Physical Processes in Hypervelocity Impact and Penetration," *High Velocity Impact Phenomena*, eds. Kinslow & Cable, Academic Press, 1970.

substrate confirming the theoretical prediction of SPAM.



**Figure 15. Deposition of 20 micron particles on an aluminum substrate**

Scanning electron microscopy was utilized to further investigate the interface between the copper deposit and the aluminum substrate to determine the extent of mixing. Metallographic cross sections were utilized for this analysis. Figure 16 represents an SEM image of the area to be mapped. The darker region is the aluminum substrate and the lighter areas the copper deposit, as denoted. Figure 17 shows the results of an x-ray map of copper while Figure 18 shows the x-ray map obtained for aluminum.

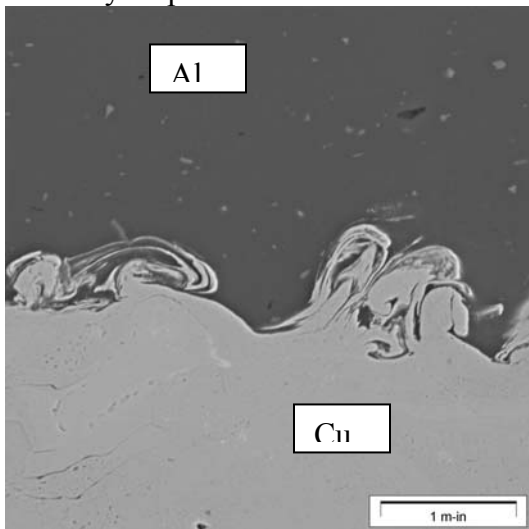


**Figure 16 SEM of copper SPD coating.**

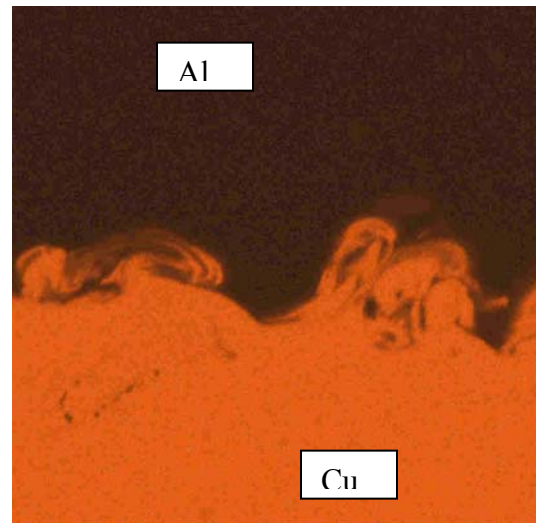


**Figure 17. X-ray map of copper.**

The maps also indicate forced mixing or SPAM to a larger extent than what can be observed in normal optical or scanning electron images.

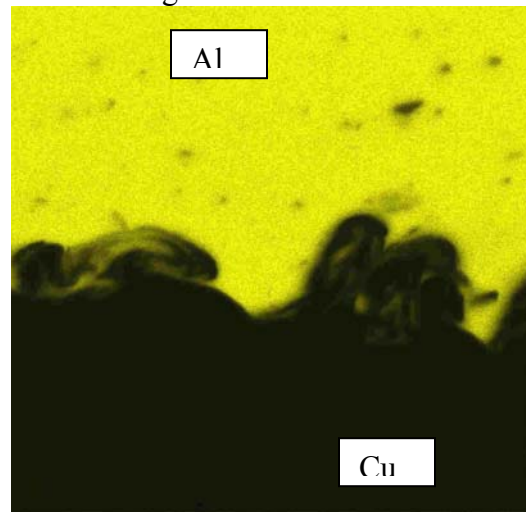


**Figure 18. X-ray map of aluminum.**

### Conclusions

- Supersonic particle deposition can yield an exceptionally strong bond between copper and Al 6061-T651.
- The phenomena occurring at the copper/aluminum interface can be characterized as “Super Plastic Agglomerate Mixing”.

- High velocity impact yields plastic deformation and viscous mixing at the particle/substrate interface.
- The resulting bond exhibits shear resistance greater than the shear strength of the copper coating.

### **Final Remarks**

It has been shown that Supersonic Particle Deposition offers real advantages over conventional thermal spray techniques. The challenge is to develop applications for SPD that can utilize these advantages economically and to demonstrate them to industry.

### **References**

1. Nobili, "Explosive Bond Process", Nobelclad Technical Bulletin NT 200, 2002
2. M. Grujicic, J. Saylor, D. Beasley, W. DeRosset and D. Helfritch, "Computational Analysis of the Interfacial Bonding between Feed-Powder Particles and the Substrate in the Cold-Gas Dynamic-Spray Process", Applied Surface Science, accepted for publication, April 2003.
3. R. J. Eichelberger and J. W. Gehring, "Effects of Meteoroid Impacts on Space Vehicles," ARS J., Vol. 32, No. 10, October 1963, p. 1583
4. R. L. Bjork, "Review of Physical Processes in Hypervelocity Impact and Penetration," High Velocity Impact Phenomena, eds. Kinslow & Cable, Academic Press, 1970.